

Absolute Proper Motion of the Canis Major Dwarf Galaxy Candidate

Dana I. Dinescu^{1,2}, David Martínez-Delgado^{3,4}, Terrence M. Girard¹, Jorge Peñarrubia³, Hans-Walter Rix³, David Butler³, and William F. van Altena¹

ABSTRACT

We have measured the absolute proper motion of the candidate Canis Major dwarf galaxy (CMa) at $(l, b) = (240^\circ, -8^\circ)$. Likely main-sequence stars in CMa have been selected from a region in the color-magnitude diagram that has very little contamination from known Milky Way components. We obtain $\mu_l \cos b = -1.47 \pm 0.37$ and $\mu_b = -1.07 \pm 0.38$ mas yr⁻¹, on the ICRS system via Hipparcos stars. Together with the radial velocity of 109 km s⁻¹, and the assumed distance of 8 kpc, these results imply a space motion of $(\Pi, \Theta, W) = (-5 \pm 12, 188 \pm 10, -49 \pm 15)$ km s⁻¹. While CMa has in-plane rotation similar to the mean of thick disk stars, it shows significant (3σ) motion perpendicular to the disk, and differs even more (7σ) from that expected for the Galactic warp. The W velocity lends support to the argument that the CMa overdensity is part of a satellite galaxy remnant.

Subject headings: galaxies: individual (Canis Majoris) — galaxies: dwarf

1. Introduction

The Sloan Digitized Sky Survey team discovered a low-metallicity ($[\text{Fe}/\text{H}] \sim -1.6$), low-Galactic-latitude structure toward the constellation of Monoceros that extends over 50 degrees in the sky, at ~ 20 kpc-distance from the Galactic center (Newberg et al. 2002,

¹Astronomy Department, Yale University, P.O. Box 208101, New Haven, CT 06520-8101 (dana@astro.yale.edu, girard@astro.yale.edu, vanalten@astro.yale.edu)

²Astronomical Institute of the Romanian Academy, Str. Cutitul de Argint 5, RO-75212, Bucharest 28, Romania

³Max-Planck Institute für Astronomie, Heidelberg, Germany (jorpega@mpia.de,rix@mpia.de, butler@mpia-hd.mpg.de)

⁴Instituto de Astrofísica de Andalucía (CSIC), Granada, Spain (ddelgado@iaa.es)

Yanny et al. 2003). Subsequent observations by Ibata et al. (2003) show that this structure extends over 100 degrees, in a ring-like configuration with distances between 15 and 20 kpc from the Galactic center. Using 2MASS M-giant tracers, Rocha-Pinto et al. (2003) confirmed the previous findings, and indicated the presence of a metal rich population ($[Fe/H] \sim -0.5$) as well. This “Monoceros (Mon) stream” is believed to be the tidal stream of a disrupting and merging dwarf galaxy. Evidence in favor of this picture are the spatial distribution and the velocity dispersion of stars in the stream (Crane et al. 2003).

Martin et al. (2004a) discovered a seemingly distinct stellar overdensity in the constellation of Canis Major, from the mapping of the sky with 2MASS-selected M giants. Deep color-magnitude diagrams in this region (Bellazzini et al. 2004 - B04, and Martínez-Delgado et al. 2005 - M05) show a well-defined main sequence, as well as a plume of blue stars which are believed to be main sequence stars younger (1-2 Gyr) than the main population of the overdensity (4-10 Gyr). Martin et al. 2004a suggest that the Canis Major overdensity is the core of the progenitor of the Mon stream. Located at $(l, b) = (240^\circ, -8^\circ)$, this overdensity has also been interpreted as due to the Milky Way warp and flare by Momany et al. (2004). These authors used UCAC2 (Zacharias et al. 2004) proper motions to argue that the motion of the CMa overdensity is indistinguishable from that of the thin disk. However, the uncertainty in the UCAC2-derived mean motion ($\sim 2 \text{ mas yr}^{-1}$) is a weak discriminant among these hypotheses. Peñarrubia et al. (2005, P05) have performed N-body simulations constrained by the available spatial and kinematical information for the Mon stream to test whether CMa is the progenitor of the Mon stream. They could only determine that CMa is a plausible, perhaps even likely progenitor of the Mon stream. While the narrowness of the main sequence of the CMa overdensity (B04 and M05) and the radial velocities in CMa (mean and dispersion, Martin et al. 2004b) argue in favor of it being a dwarf remnant rather than the thin disk warp, the common origin of the Mon stream and CMa can be tested stringently with a precise measurement of its absolute proper motion¹. It is the purpose of the present work to provide such a proper-motion measurement.

2. Proper-Motion Determinations

Our proper-motion measurement is based on two photographic plate pairs that are part of the Southern Proper Motion Program (SPM, e.g., Girard et al. 2004) and on CCD ob-

¹For simplicity, we will refer to the Canis Major overdensity as the Canis Major dwarf, although we are aware that there isn’t yet consensus regarding the nature of this stellar overdensity (i.e., core of the satellite dwarf, stream of the satellite or Galactic warp).

servations made with the Wide-Field Imager (WFI) at prime focus of the 2.2m ESO/MPG telescope at La Silla Observatory in December 2003 (M05). The SPM plates were taken with the 50-cm double astrograph at Cesco Observatory in El Leoncito, Argentina (plate scale = 55.1 "/mm), in 1967 and in 1988. At each epoch, two plates are taken in the V and B passbands, and the area covered is $6.3^\circ \times 6.3^\circ$. The CCD data cover an area of about half a degree on a side, and they are located on a corner of the SPM field, at $(l, b) = (240.15^\circ, -8.08^\circ)$. Each SPM plate contains a two-hour exposure, which reaches to about $V = 18$, and an offset two-minute exposure, which allows a tie-in to bright reference stars. During both exposures, an objective grating is used, which produces a series of diffraction images on either side of the central zero-order image. The presence of the grating images is advantageous for two reasons: It effectively extends the dynamic range of the plates, in both the long and short exposures, providing unsaturated images of brighter stars. More importantly, the grating images provide the means for calibrating and correcting the magnitude equation in each exposure. (See Girard et al. 1998 for a detailed discussion of the techniques involved. The theory is described in Section 3 of that paper, and Section 4 describes its application to SPM plates as well as an assessment of its effectiveness.)

The photographic plates were scanned with the Yale PDS microdensitometer, at a pixel size of 12.7 microns. The preparation of the input list of stars to be measured, the PDS measurements, and the astrometric reductions are all similar to those described by Dinescu et al. (2003), Girard et al. (1998) and references therein. In the area of the plate covered by the CCD observations we measure all of the stars listed in the CCD data that are detectable on the photographic plates.

We have performed two types of proper-motion solutions that eventually are combined to produce the final result. The first one is a separate reduction of the visual and blue plate pair, and excludes the CCD observations. This determination, in principle, can provide two independent measurements of the *absolute* proper motion of CMa. However, because CMa candidate stars are faint ($V \geq 16$), their individual proper motions will have large proper-motion uncertainties (see Girard et al. 2004). As we expect only ~ 150 CMa candidates within the CCD region, their mean motion will be poorly determined. Consequently, we will use this plate-pair approach only to determine the correction to absolute proper motion via Hipparcos stars, and to tie into a new proper-motion system (see below). The second approach combines all four plates and the CCD positions to determine *relative* proper motions for the stars in the area limited by the CCD data. In this way the time baseline is extended from 21 years to 36 years with the immediate result of improving the precision of the proper motions. The “all-plate” proper-motion system is tied to each “plate-pair” proper-motion system using proper-motion offsets. These offsets are the means of the proper-motion differences between the two systems for about 1600 stars for the visual pair and 1700 stars for

the blue plate pair.

For the plate-pair solution, different-epoch plates are mapped into each other using the faint anonymous stars, and a polynomial plate model that includes only geometric terms. (Magnitude equation was corrected previous to the plate-pair solution using the techniques referenced earlier.) The correction to absolute proper motion is defined by the motion of ~ 120 Hipparcos stars with respect to the faint anonymous (reference) stars. First, the mean proper-motion of Hipparcos stars is determined for each image order (there are a total of 2 central orders for the long and short exposures and 4 diffraction orders; symmetric positions of the same order are averaged). The final value for each plate pair is a weighted mean of all image-order values. The weights are given by the internal scatter within each image order. For the blue plate pair we obtained $\mu_\alpha \cos \delta = -1.30 \pm 0.24$ and $\mu_\delta = 3.34 \pm 0.36$ mas yr $^{-1}$. For the visual plate pair we obtained $\mu_\alpha \cos \delta = -1.79 \pm 0.19$ and $\mu_\delta = 0.90 \pm 0.19$ mas yr $^{-1}$. We note that the blue and visual values need not be in agreement since, on average, different faint reference stars were used in each plate-pair solution.

The all-plate solution combined all positions in one proper-motion solution, in an iterative process (e.g., Girard et al. 1989). The CCD data are from 8 individual chips of the WFI, which were independently reduced into the photographic plates. Formal individual uncertainties increase with magnitude from 1.4 mas yr $^{-1}$ at $V \sim 12$ -15 up to 4 mas yr $^{-1}$ at $V \sim 17.5$. The proper-motion offsets between the system of the all-plate solution and that of the blue plate pair are: $\mu_\alpha \cos \delta = -0.12 \pm 0.12$ and $\mu_\delta = -1.96 \pm 0.11$ mas yr $^{-1}$. Similarly, for the visual plate pair we obtain: $\mu_\alpha \cos \delta = 0.32 \pm 0.13$ and $\mu_\delta = 0.47 \pm 0.13$ mas yr $^{-1}$. The final correction to be applied to the relative proper motions of the all-plate system in order to transform them to absolute proper motions is the sum of the system offsets and the proper motions of Hipparcos stars with respect to a given plate-pair reference system. These summed corrections are: for the blue plate pair, $\mu_\alpha \cos \delta = -1.42 \pm 0.27$, $\mu_\delta = 1.38 \pm 0.38$ mas yr $^{-1}$, and for the visual plate pair, $\mu_\alpha \cos \delta = -1.47 \pm 0.23$, $\mu_\delta = 1.37 \pm 0.23$ mas yr $^{-1}$. We take the error-weighted average of the two determinations as the final value of the correction to absolute proper motion of the all-plate system. This is $\mu_\alpha \cos \delta = -1.45 \pm 0.18$, $\mu_\delta = 1.37 \pm 0.20$ mas yr $^{-1}$. Here we assume that the two determinations are independent, although strictly speaking they are not, because the system proper-motion offsets are highly correlated. However, the dominant source of uncertainty comes from the Hipparcos tie-in measurement which is determined independently from two plate-pairs.

3. Absolute Proper Motion of CMa

In Figure 1 (top panel) we show the color-magnitude diagram (CMD) for all stars from M05 that were successfully measured on the photographic plates. The photometry is that from M05. The bottom panel of Fig. 1 shows a simulated CMD from the Besançon Galactic model (Robin et al. 2003) in the area of the sky covered by the CCD observations. This model includes the stellar warp as characterized from preliminary results from the DENIS survey (Epchtein et al. 1997). Two regions of interest are marked in each panel: the “blue plume” (BP) region likely representing the upper main sequence of a younger sub-population in CMa, with very little Milky-Way contamination, and the “red-clump” (RC) region of CMa ($1.4 \leq B - R \leq 1.8$, and $14.5 \leq R \leq 16$). These regions are described in detail below.

There is a $B - R$ color offset of 0.19 between the observations and the model in the sense that the simulated data are redder than the observations. This may be attributed to the particular reddening used in the Besançon Galactic model. Consequently, we have shifted the simulated data by this offset. The model data are used only for a qualitative understanding of the expected Galactic populations and not a quantitative comparison. The overall shapes of the CMDs are similar. Toward the red end, the incompleteness of the observations is apparent when compared to the Galactic model. Bright stars ($R < 14.5$) are also missing from Fig. 1, top panel, as they were saturated in the initial input list derived from CCD data. The main difference between the observations and the Galactic model are the blue, faint stars ($16 < R < 18$, and $B - R \leq 0.8$) already noted by B04 and M05. As in the above-mentioned papers, we will refer to it as the blue plume (BP). For magnitudes brighter than $R \sim 16$, there is a significant number of stars in the Galactic model, blueward of the halo/thick disk main sequence turn-off. According to the model, these are 2-3 Gyr-old main sequence stars at distances $\sim 2 - 4$ kpc. Their model velocities indicate that they belong to a thin-disk like population.

To avoid Galactic star contamination, we have drawn a polygon (highlighted in Fig. 1, top panel) guided by the configuration of the Galactic-model CMD. Only stars within this polygon were considered in the proper-motion determination, and these are the candidate BP stars of CMa. Previous attempts to estimate the motion of CMa from radial velocities, proper motions and the spatial configuration (e.g., Momany et al. 2004, Martin et al. 2004b, P05 and references there in) indicate that its orbit is prograde and not highly inclined with respect to the disk. If this is the case, the proper motion of CMa will overlap with the proper-motion distribution of distant disk stars that will have small proper motions and a low proper-motion dispersion. Samples that include both CMa stars and Galactic disk stars, such as the red clump region (RC) of CMa (see Fig. 1) and the giant branch of CMa seen in the 2MASS studies, will be subject to proper-motion bias from the disk stars. To

illustrate, in Figure 2 we show the absolute proper-motion distribution of the observations (top) and of the Galactic model predictions (bottom) in the CMa red-clump region of the CMD. The Galactic-model proper motions were convolved with proper-motion uncertainties that mimicked those of our observations. The two distributions are similar, and it is difficult to decide if a kinematically distinct population is present in the observations that is not in the Galactic model. In the model, the stars that appear to clump (i.e., have a proper-motion dispersion comparable to the proper-motion uncertainties) are primarily ~ 5 Gyr-old disk giants at distances between 3 and 8 kpc. It is this population that will bias the CMa proper motion in samples that use this portion of the CMD. Therefore it is crucial to select photometrically a clean sample of CMa candidates to determine the proper motion.

In Figure 3 we show the absolute proper motions of CMa candidates selected from the BP polygon region in Fig. 1. The single-coordinate proper-motion error estimates vary from 2.2 to 4.1 mas yr⁻¹ as a function of magnitude, with a mean value of 3.1 mas yr⁻¹. Also shown are the proper-motion marginal distributions along the two axes. We have chosen to use a trimmed mean to estimate the average motion because of the apparent presence of outliers. Probability plots (Lutz & Uppgren 1980) indicate that the inner 80% of the sample is roughly Gaussian. This corresponds to 104 (of the total 130) stars within 8 mas yr⁻¹ of the tentative mean, limits that also appear reasonable based on the appearance of the marginal distributions. From these 104 stars, the mean absolute proper motion of CMa is $\mu_\alpha \cos \delta = -1.61 \pm 0.38$, $\mu_\delta = 0.84 \pm 0.37$ mas yr⁻¹. In Galactic coordinates, it is $\mu_l \cos b = -1.47 \pm 0.37$, $\mu_b = -1.07 \pm 0.38$ mas yr⁻¹. The quoted uncertainties include the contribution from the correction to absolute proper motion. The dominant source of uncertainty is the determination of the mean for these faint BP stars. The estimated mean is indicated in Figure 3 by the intersecting solid lines.

4. Discussion

Taking the distance to the CMa core to be 8.1 ± 0.4 kpc (M05, B04), and the radial velocity to be 109 ± 4 km s⁻¹ (Martin et al. 2004b), we obtain the velocity with respect to the Galactic rest frame in cylindrical coordinates: $(\Pi, \Theta, W) = (-5 \pm 12, 188 \pm 10, -49 \pm 15)$ km s⁻¹. Assumptions include the peculiar Solar motion from Dehnen & Binney (1998), that the Sun is located at 8.0 kpc from the Galactic center (GC), and the rotation of the local standard of rest is 220.0 km s⁻¹. Martin et al. (2004b) determine two peaks in the radial velocity distribution of M giants in CMa. Both peaks have a low radial velocity dispersion (i.e., 9 and 13 km s⁻¹), indicative of a common-motion, cold system. We adopt the mean of the most populated peak as the radial velocity of the CMa dwarf. P05 models also favor this

value, while the second peak may be due to a tidal tail surrounding CMa. In the Galactic rest frame, the proper motion is: $\mu_l \cos b' = -4.16 \pm 0.37$, $\mu_b' = -1.61 \pm 0.38$ mas yr⁻¹.

Momany et al. (2004) suggest that the warping of the disk is responsible for the CMa overdensity. The geometry of the stellar warp and flare have been recently parameterized by López-Corredoira et al. (2002). The line of nodes of the warp is $\sim 5^\circ$ away from the GC-Sun direction, in the sense of Galactic antirotation. The maximum deflection below the Galactic plane is in quadrant 4, and above the plane in quadrant 1 (see Fig. 22 in López-Corredoira et al. 2002). In quadrant 3, where CMa is located, material from the warp is moving from below the plane, up toward the plane, i.e., with a positive W velocity. Following Drimmel, Smart & Lattanzi (2000, D00), where the kinematic signature of the warp is derived for a traditional, long-lived Galactic warp, (their equations 5 and 11, and no precession), we obtain $W_{warp} = 52$ km s⁻¹. In order to obtain a negative W velocity, D00 had to invoke an unphysically high precession rate for the warp. Our W velocity component is inconsistent (7σ) with the expected motion of the warp at this Galactic location. If there is no warp, then the W velocity of CMa is 3.3σ different from the velocity of the thin disk. The motion of the warp as estimated above, $(\Pi, \Theta, W) = (0, 220, 52)$ km s⁻¹, translates into $\mu_l \cos b' = -4.95$, $\mu_b' = 0.95$ mas yr⁻¹, at the CMa distance. The hypothetical warp motion, transformed to celestial coordinates, is indicated in Figure 3 as the intersecting dotted lines.

By integrating the orbit in the Johnston, Spergel & Hernquist (1995) Galactic potential model, we obtain a pericenter of 10.5 ± 0.9 kpc, and an apocenter of 14.0 ± 0.2 kpc. The maximum distance from the Galactic plane is 2.0 ± 0.4 kpc, and the orbital period is 342 ± 14 Myr. The orbit inclination is $15^\circ \pm 3^\circ$ and the eccentricity is 0.14 ± 0.04 . The uncertainties in the orbital elements were derived in a Monte Carlo fashion from the uncertainties in the distance, radial velocity and proper motions (Dinescu, Girard & van Altena 1999). The derived motion makes CMa a likely parent of the Mon stream as envisioned by P05. Indeed, their modeling gives an orbital inclination of $20^\circ \pm 5^\circ$, and an eccentricity of 0.10 ± 0.05 for the Mon stream progenitor. Currently, CMa is at apocenter, and N-body simulations show that it should undergo tidal disruption (P05). The original orbit of the progenitor seems to have been highly coupled with the disk motion, i.e., a prograde, low-inclination orbit of low eccentricity. Therefore the interaction with the disk could have altered the orbit of the progenitor for instance, by decreasing the initial orbital inclination (Walker, Mihos & Hernquist 1996). Likewise, this interaction may have altered the shape of the disk, perhaps inducing the existent warp.

We acknowledge funding from the National Science Foundation, grant AST-0407293.

REFERENCES

- Bellazzini, M., Ibata, R., Monaco, L., Martin, N., Irwin, M. J., & Lewis, G. F. 2004, MNRAS, 354, 1263 (B04)
- Crane, J. D., Majewski, S. R., Rocha-Pinto, H. J., Frinchaboy, P. M., Skrutskie, M. F., & Law, D. R. 2003, ApJ, 594, L122
- Dehnen, W. & Binney, J. 1998, MNRAS, 298, 387
- Dinescu, Girard, & van Altena 1999, ApJ, 117, 1792
- Dinescu, D. I., Girard, T. M., van Altena, W. F., & López, C. E. 2003, AJ, 125, 1373
- Drimmel, R., Smart, R. L., & Lattanzi, M. G. 2000, A&A, 354, 67 (D00)
- Epchtein, N., et al. 1997, The Messenger, 87, 27
- ESA 1997, The Hipparcos and Tycho Catalogues (ESA SP-1200) (Noordwijk: ESA)
- Girard, T. M., Grundy, W. M., López, C. E., & van Altena, W. F. 1989, AJ, 98, 227
- Girard, T. M., Platais, I., Kozhurina-Platais, V., van Altena, W. F., & López, C. E. 1998, AJ, 115, 855
- Girard, T. M., Dinescu, D. I., van Altena, W. F., Platais, I., Monet, D. G. & López, C. E. 2004, AJ127, 3060
- Johnston, K. V., Spergel, D. N., & Hernquist, L. 1995, ApJ, 451, 598
- Lasker, B. M., Sturch, C. R., McLean, B. J., Russell, J. L., Jenker, H., & Shara, M. 1990, AJ, 99, 2019
- López-Corredoira, M., Cabrera-Lavers, A., Garzón, F., & Hammersley, P. L. 2002, A&A, 394, 883
- Lutz, T. E. & Upgren, A. R. 1980, AJ, 85, 1390
- Martin, N. F., Ibata, R. A., Bellazzini, M., Irwin, M. J., Lewis, G. F., & Dehnen, W. 2004a, MNRAS, 348, 12
- Martin, N. F., Ibata, R. A., Conn, B. C., Lewis, G. F., Bellazzini, M., Irwin, M. J., & McConnachie, A. W. 2004b, MNRAS, 355, L33
- Martínez-Delgado, D., Butler, D. J., Rix, H. W., Franco, Y. I., & Peñarrubia, J. 2005, ApJ, in press, (M05)
- Momany, Y., Zaggia, S. R., Bonifacio, P., Piotto, G., De Angeli, F., Bedin, L. R., Carraro, G. 2004, A&A, 421, L29
- Newberg, H. J. et al. 2002, ApJ, 569, 245

- Peñarrubia, J., Martínez-Delgado, D., Rix, H. W., Gómez-Flechoso, M. A. Munn, J., Newberg, H., Bell. E. F., Yanny, B., Zucker, D. & Grebel, E. K. 2005, ApJ, in press (P05)
- Rocha-Pinto, H.J., Majewski, S. R., Skrutskie, M. F. & Crane, J. D. 2003, ApJ, 594, L115
- Yanny, B. et al. 2003, ApJ, 588, 824
- Walker, I. R., Mihos, C. J., & Hernquist, L. 1996, ApJ, 460, 121
- Zacharias, N., Urban, S. E., Zacharias, M. I., Wycoff, G. L., Hall, D. M., Monet, D. G., & Rafferty, T. J. 2004, AJ127, 3043

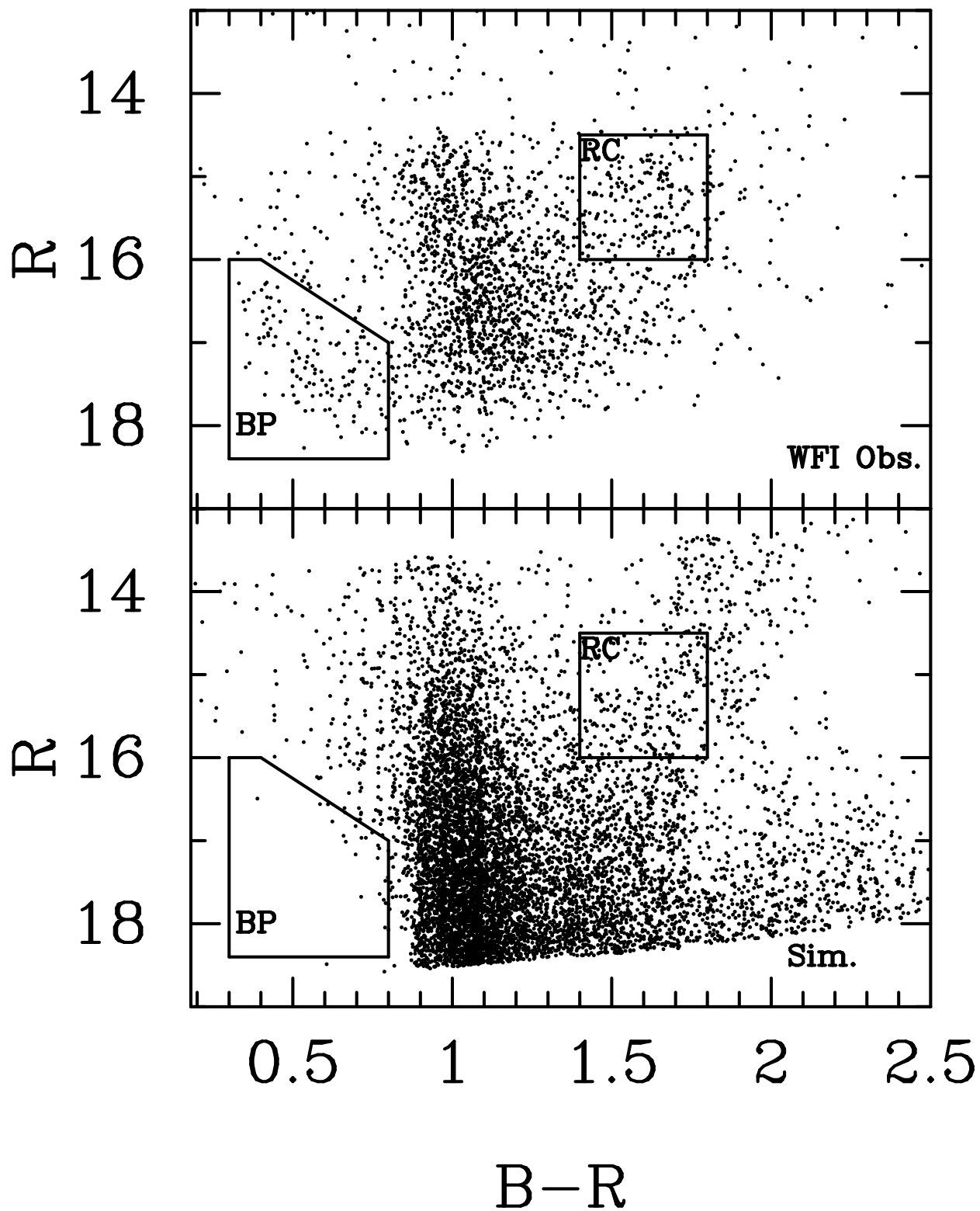


Fig. 1.— Color-magnitude diagrams of the stars observed in the CMa region with proper-motion measurements (top), and the simulations of known Milky-Way components (bottom). The blue-plume region and the red-clump region are marked. A 0.19 $B - R$ color shift has been applied to the simulated data (see text).

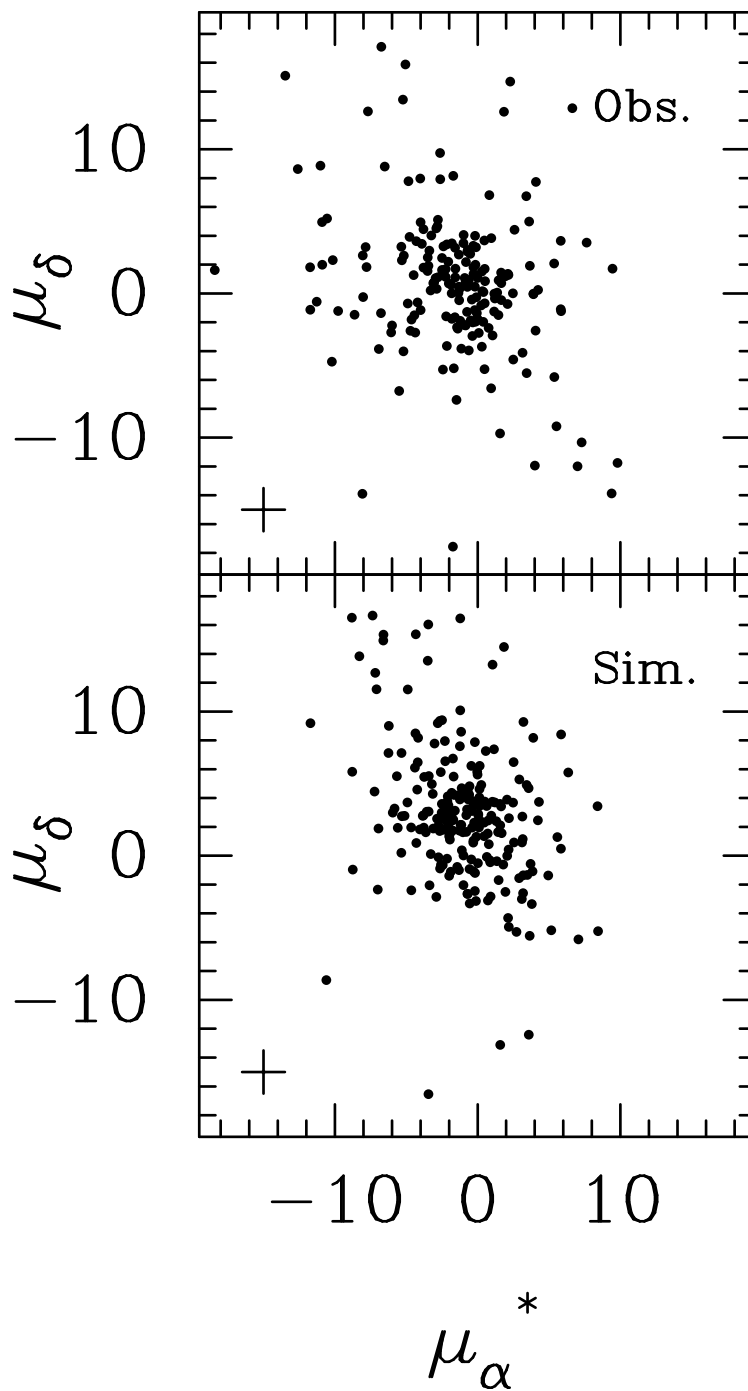


Fig. 2.— Vector-point diagram of stars in the red-clump region of CMa. Observations are shown in the top panel, simulated data for the smooth Milky Way components in the same direction are shown in the bottom panel ($\mu_\alpha^* = \mu_\alpha \cos \delta$). Typical proper-motion uncertainties are indicated in each panel. It is apparent that CMa stars can not be separated from disk stars, on the basis of proper motions alone.

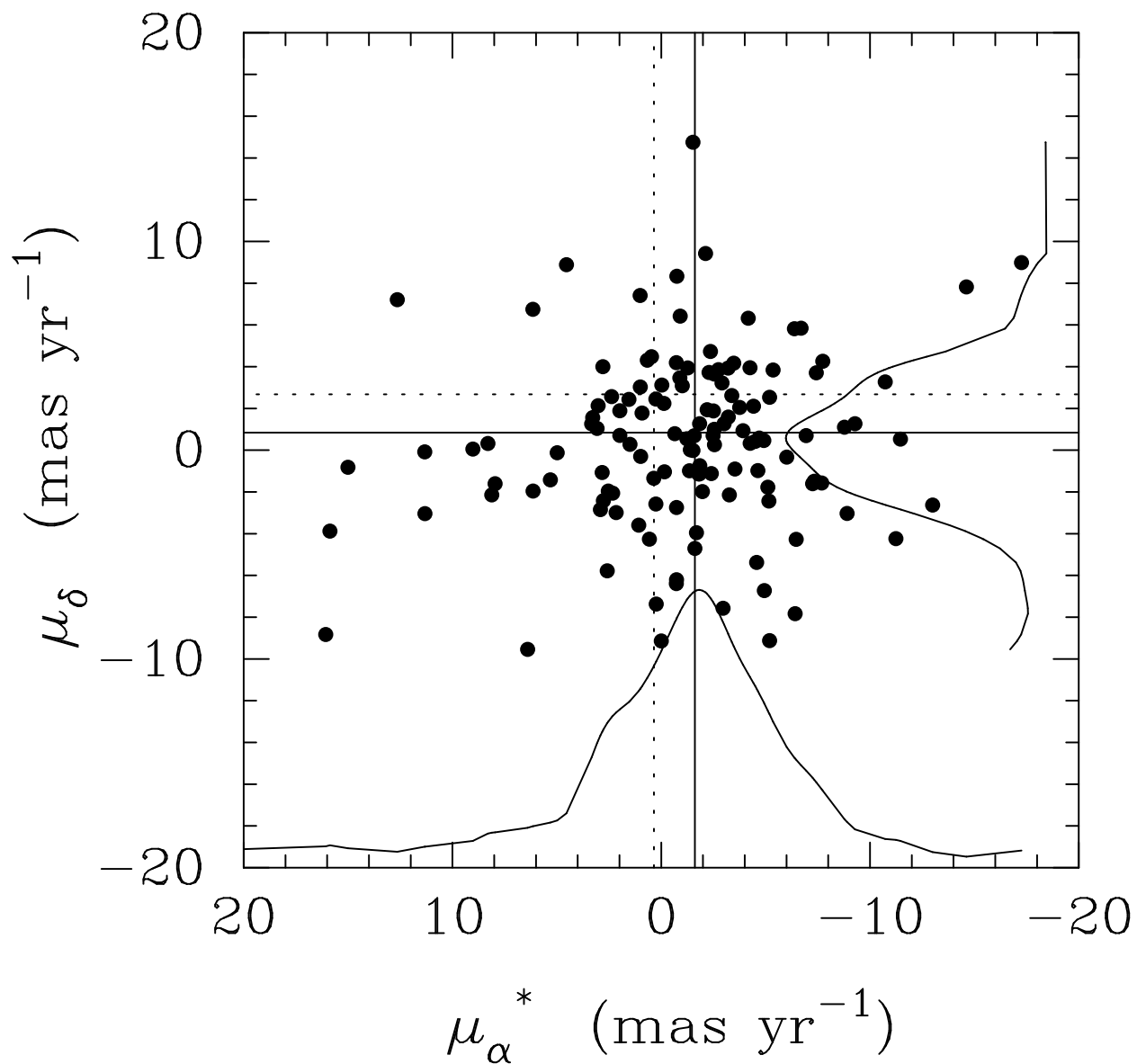


Fig. 3.— Absolute proper-motion vector-point diagram of the CMA blue-plume candidates. One-dimensional marginal distributions, also shown, were constructed by convolving with a 1 mas yr⁻¹ Gaussian kernel. The intersecting solid lines indicate the estimated mean motion of the sample. The dotted lines indicate the expected motion of the Galactic warp at this position.